

# Ultracapacitor model with automatic order selection and capacity scaling for dynamic system simulation

R.A. Dougal, L. Gao\*, S. Liu

*Department of Electrical Engineering, University of South Carolina, Columbia, SC 29208, USA*

Received 23 July 2003; accepted 14 August 2003

## Abstract

An ultracapacitor model with automatic order selection of complexity and automatic scaling of capacity is created in Virtual Test Bed platform for complex system simulation and prototyping. The order selection is based upon the variable simulation time step for appropriate level of details of the model, and automatically executed by the model itself, therefore it applies to simulation for both high and low frequencies, or for both fast and slow transients, or even for multi-time scale resolutions. A simple trapezoidal algorithm, rather than the general stiff algorithm, which is complicated in implementation, is used for numerical integration. For a given time step, the truncation error is controlled to be negligible, so that numerical stability and accuracy are ensured for the given order of model complexity. The model is validated by comparing the simulation results to the experimental ones. The application example of the ultracapacitor model in complex system simulation is also presented.

© 2003 Elsevier B.V. All rights reserved.

*Keywords:* Automatic order selection; Impedance spectroscopy; Ladder model; Ultracapacitors; Variable time-step simulation; Virtual Test Bed

## 1. Introduction

An ultracapacitor or an electrochemical capacitor, or a double layer capacitor [1] can have much greater charge or energy storage than a conventional capacitor because of its highly-amplified surface area of micropore-structured electrodes. For the same reason, an ultracapacitor exhibits operating characteristics that are distinct from those of a conventional capacitor. In particular, its volt-second relation is nonlinear, and its impedance is a complicated function of frequencies. The peculiarities of the ultracapacitor characteristics arise from the charge (anions and cations) transport process in porous electrodes (activated carbon or other carbon-based pore materials), which is subject to limitations from both mass transfer and Faradaic process that earned it the name of the electrochemical capacitor. Depending upon the constructions of porous electrodes, the characteristics of ultracapacitors can vary significantly due to different charge and current distributions determined by the pore structures and materials of the electrodes.

Many models for ultracapacitors were developed, among which is a widely used one that was based on the porous

electrode theory [2–4]. The model solves diffusion equations with respect to the charge species transport in the matrix phase of electronically conductive pores and an ionically conductive electrolyte. The time-domain solution of the model under a galvanostatic discharge is a combination of a series of transients characterized by different time constants determined by parameters of micropore structure and material properties. From the stand point of modeling and simulation, the significance of the model based on the porous electrode theory is that it reveals how the operating characteristics of ultracapacitors are affected by charge transport process for given electrode materials and structures. In particular, an equivalent circuit based on the transients can be constructed to synthesis the model characteristics, with each transient being specified by a time constant generated from a resistor–capacitor branch. Specifically, a cascaded multi-stage resistor–capacitor ladder model can be derived for the ultracapacitor model. Depending upon the accuracy requirement, the transient terms can be truncated to an appropriate number so that the computation effort can be minimized for a given accuracy. Correspondingly, the number of stages in the ladder model can be truncated for the same reason.

The ladder model derived by Miller et al. [5,6] was based on the impedance spectroscopic measurement. The values for the resistors and capacitors and the ladder network can be

\* Corresponding author. Tel.: +1-803-777-9314; fax: +1-803-777-8045.  
E-mail address: [gaolijun@engr.sc.edu](mailto:gaolijun@engr.sc.edu) (L. Gao).

viewed as a circuit-parameterized charge transport in porous electrodes of ultracapacitors. In particular, the five-stage ladder model has a sufficient accuracy for most applications, accounting for the frequency range up to 10 kHz, or a transient of a time constant about 100  $\mu$ s. However, the five-stage ladder model is often inconvenient in simulation if the system characterization concerns low frequencies or a large time constant only, since it simply takes too much time to calculate unnecessary details. In this case, a lower order or fewer stages in the ladder are needed. Of course, a separate model can always be made to serve the purpose, but our model presented in the paper is aimed to solve the problems concerning multi-time scale resolutions with a single model.

The model presented here is based on the five-stage ladder model for the Maxwell PC100 module, and it is built in the Virtual Test Bed [7] computational environment for complex engineering system simulation and prototyping. The primary features of the model include: (1) automatic selection of the order or number of stages of the ladder network according to the simulation time step; (2) scaled values for resistors and capacitors in the network when the network order advances or reduces in order to minimize the error; (3) automatic selection of the network order according to the frequency input by users and recommendation of appropriate simulation time step; and (4) total capacity scaling based on the 100 F module.

In the following section, we will describe the model first with respect to the numerical accuracy and stability, the relations of the order to the time step size, and the auto-order selection method. Then in Section 3, the simulation of the ultracapacitor in an electric hybrid vehicle is illustrated. The conclusions are given in the final section.

## 2. Model description

The equivalent circuit of the multi-stage ladder model [5,6,8] for ultracapacitor is shown in Fig. 1. The reasons we use this circuit are: (1) it physically mimics the distributed nature of the ultracapacitor, and its performance fits the experimental data very well within a wide range of frequencies; (2) it can be easily combined with various loads and used to find analytical or numerical solution; and (3) the network is easy to adopt order reduction method as the energy storage components in the multi-stage ladder from left to right in turn represent the complex transient processes from fast speed to slow speed in ultracapacitors. Notice that the model

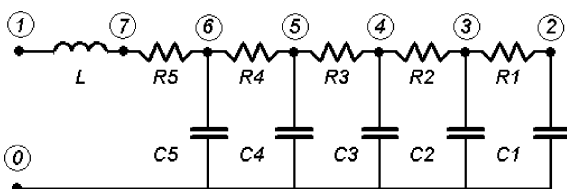


Fig. 1. Equivalent circuit of ultracapacitors.

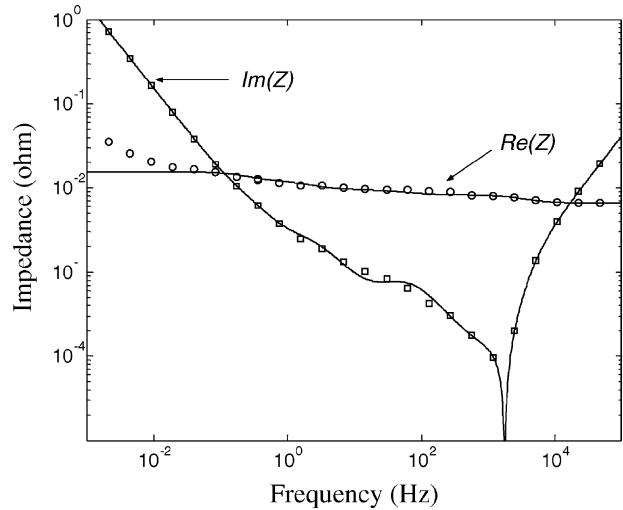


Fig. 2. Comparison of the model predictions of impedance with the measurements. The simulation results are indicated by lines and the measurements are by squares and circles.

contains actually six energy-storage elements (including the stray inductance), therefore yielding six state variables. The corresponding differential equation will be of six orders. However, for the convenience of discussing order reduction, we will use the word order and the stage interchangeably. For example, order reduction means reducing the number of stages. In Fig. 2, the comparison of the impedance obtained from the equivalent ladder model (as in Fig. 1) and from the measurements [8] is shown for the Maxwell 100 F ultracapacitor. The parameters for the model, as given by Table 1, were obtained by using nonlinear least-squares (CNLS) fitting routine applied to the measured data. It can be concluded from Fig. 2 that there is a good agreement between the ladder model and the experimental data in a wide range of frequencies. Also it can be seen that the imaginary part of impedance changes remarkably as the frequency varies while the real part keeps relatively constant.

### 2.1. Numerical oscillation

Typical solution techniques for differential equations in most of the time-domain circuit simulators are trapezoidal or implicit Euler or Gear’s algorithm, and others. The Virtual Test Bed offers flexibility for model developers to apply any of those within their models based on the considerations for accurate and fast computation. Since the

Table 1  
Model parameters of Maxwell 100 F

$R_5$	0.00662 $\Omega$	$C_5$	0.0281 F
$R_4$	0.0017 $\Omega$	$C_4$	2.05 F
$R_3$	0.00147 $\Omega$	$C_3$	18.9 F
$R_2$	0.00494 $\Omega$	$C_2$	53.2 F
$R_1$	0.0296 $\Omega$	$C_1$	31.7 F
$L$	6.5E-8 H		

trapezoidal method is absolute order stable, and provides a good compromise among simplicity and accuracy, it is one of the favorite methods used in VTB model developing.

However, numerical oscillations can occur under some circumstances. The numerical oscillations can be classified into two types. The first type of numerical oscillation is caused by step change in certain state variables. Several approaches have been proposed to solve this type of numerical oscillation [9–11]. The second type of numerical oscillation arises from an inappropriate time step size. Generally, the second type of numerical oscillation can be avoided by reducing the simulation time step; however, unnecessary small simulation time steps will dramatically increase the computational effort. Clearly, it is necessary to choose an appropriate time step for better accuracy and faster computation while avoiding erroneous oscillation. This paper focuses on the second type of numerical oscillation in modeling and simulation of the ultracapacitor having multiple constants, and provides an effective method to choose appropriate step size for sufficient computation accuracy while minimizing computation time.

Let us consider a simple case first, a circuit including a capacitor and a resistor, as shown in Fig. 3, which may be one of the stages of the ultracapacitor model.

The equation for the terminal current is,

$$i(t) = C \frac{dv(t)}{dt} - \tau \frac{di(t)}{dt} \quad (1)$$

where

$$\tau = R \cdot C \quad (2)$$

is the time constant of the circuit. Applying the trapezoidal rule within the time interval  $(t, t - h)$ , where  $h$  is the time step, and rearranging, we obtain,

$$i(t) = g \cdot v(t) - b(t - h). \quad (3)$$

where,

$$g = \frac{2C}{2\tau + h}, \quad (4)$$

$$b(t - h) = \frac{2C}{2\tau + h} v(t - h) - \frac{2\tau - h}{2\tau + h} i(t - h) \quad (5)$$

are the admittance and the current history respectively. The current history is dependent of the values of the terminal

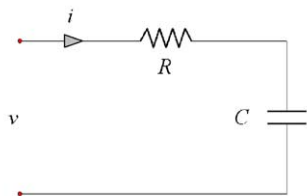


Fig. 3. A first order equivalent circuit of an ultracapacitor.

voltage and the current at the previous step. The following recursion equation can be obtained using Eqs. (3) and (5),

$$i(nh) = \left( \frac{2\tau - h}{2\tau + h} \right)^n i(0) + g \cdot \sum_{k=1}^n \left\{ \left( \frac{2\tau - h}{2\tau + h} \right)^{(n-k)} [v(kh) - v((k-1)h)] \right\}, \quad (6)$$

$$k = 1, 2, \dots, n,$$

where  $nh = t$ . The criteria for Eq. (6) to be numerically stable is

$$h > 0, \quad \tau > 0 \quad (7)$$

which can always be satisfied. However, if  $h = 2\tau$ , the first term in Eq. (6) yields zero. If  $h > 2\tau$ , the sign of the first term in Eq. (6) changes from one time step to the next, therefore, causing the current value to oscillate. The second term contributes oscillations too, since the sign of the voltage at the  $k$ th step also changes every time  $n$  advances.

For the ultracapacitor model shown in Fig. 1, there are total six equivalent time constants, corresponding to six energy-storage elements, widely spreading from micro-seconds to seconds. If the model is used in simulation of a system of line-frequency or lower frequencies, the time step must be smaller than two times of smallest time constant of the ultracapacitor, which is in micro-seconds in order to prevent numerical oscillations. For example, Fig. 4 shows the numerical oscillations of the ultracapacitor model with an inappropriate simulation time step (here using 0.005 s) when it is connected to an ideal voltage source (1 V). It is clearly seen that the currents of  $C_5$  and  $C_4$  oscillate heavily from about  $-100$  to  $100$  A and decline slowly.

Also apparent is that the currents  $C_1$  and  $C_2$  look much better, which means for a fixed circuit model, a given simulation time step will mainly affect different stages. So the oscillation problem can be avoided if an equivalent circuit of an appropriate order or appropriate time constants is chosen based on the characterization time of the system inputs, as illustrated in the next subsections.

## 2.2. Order reduction method

As shown in Fig. 5, four different ladder networks are embedded into one ultracapacitor model. The model will choose the appropriate circuit according to the simulation time step. For example, to reduce from the five-order to the four-order, the 4th order capacitor value in the four-order network is substituted by the  $C_5 + C_4$  value in the five-order circuit. The same procedure is repeated for the resistor in the four-order circuit. Note the inductor is just ignored in the low frequency band. A close look at the value of capacitor and the resistor in the two-order shows they are the summation of all parameter values in the five-order. The five-order circuit is not preferred, since it is too simple and yields too big error.

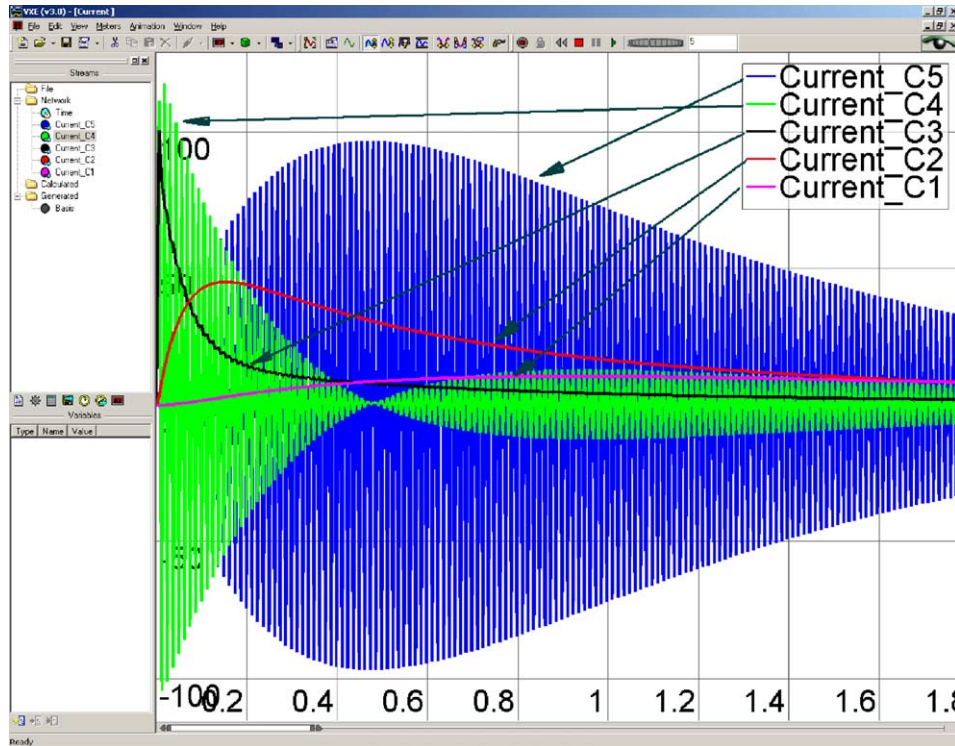


Fig. 4. Numerical oscillation due to an inappropriate simulation time step.

Note that the circuit topology for each order is not unique as it is always somewhat arbitrary when modeling a two-terminal device with more than two internal elements. The topologies we choose, as shown above, are simply inherited from the original one, and they are degraded to a smaller RC network each time an order is reduced. We believe that the network will best represent the nature of the charge processes in the ultracapacitor, as illustrated by the Fig. 2 and subsequent figures.

2.3. Determination of maximum time step for each order

In this section, the equivalent circuit model in Fig. 1 is first analyzed. Then the definition of the simulation time step  $T_{Ref}$  is proposed; after that, the model with different order networks as shown in Fig. 5 is studied with consideration to simulation time step selection.

First, let us consider the circuit shown in Fig. 1, it is not obvious how to calculate the equivalent time constants associated with each independent energy storage component since all the components are coupled together. However, the time constants can be approximated by decoupling the related resistor–capacitor stage from the network using an appropriate assumption. Let’s arbitrarily choose node 4 and assume it is the node whose variables first begin to numerically oscillate with the simulation time step increasing. Under this condition, the voltage variations of the other nodes are slower than the voltage variation of node 4. Approximate the voltages of nodes 3 and 5 ( $V_3$  and  $V_5$ ) as fixed values, which means the nodes 3 and 5 can be looked upon, as connecting to ideal voltage sources, so that the components of  $C_3$ ,  $R_2$  and  $R_3$  are decoupled from the network. The time constant of this stage resistor–capacitor is described as:

$$T_3 = C_3 \cdot \left( \frac{R_3 \cdot R_2}{R_3 + R_2} \right) \tag{8}$$

According to Eqs. (6) and (8), the maximum simulation time step for node 4 without numerical oscillation is  $2T_3$ . Repeating this process, all the time-constants of the ultracapacitor

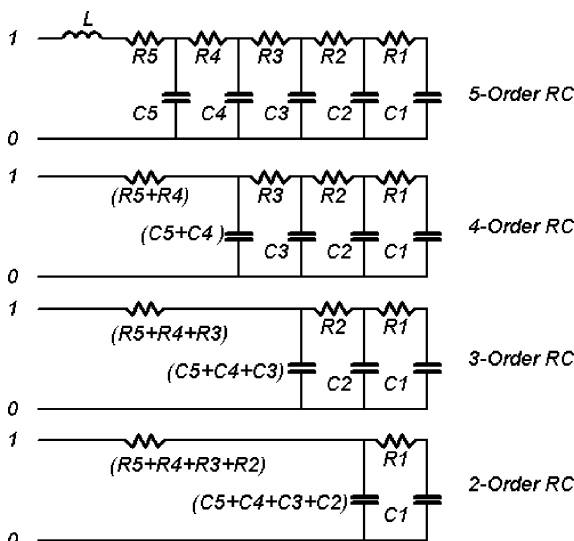


Fig. 5. Automatic order selection method.

Table 2  
Six relevant time constants of the model in Fig. 1

Related components	Time constant (s)
$T_6$ ( $R_5L$ )	9.8187E–6
$T_5$ ( $R_5R_4C_5$ )	3.80093E–5
$T_4$ ( $R_4R_3C_4$ )	0.001616073
$T_3$ ( $R_3R_2C_3$ )	0.021411548
$T_2$ ( $R_2R_1C_2$ )	0.225220521
$T_1$ ( $R_1C_1$ )	0.93832

model in Fig. 1 are obtained and listed in Table 2. From  $T_6$  to  $T_1$  in turn, the time constants increase respectively, and  $T_6$  is the smallest one, which means that the numerical oscillations will occur from the left stage to right in turn as the simulation time step increasing. This is not a coincidence but determined by the modeling method in which the left stages in the model are used to cover the fast behavior of ultracapacitors and the right stages are used to determine the long time behavior.  $2T_6$  is the maximum time step for the model in Fig. 1 from numerical oscillation; however, in order to make the simulation results represent the real world process well, the simulation time step should be at least a few times shorter than  $2T_6$ , we here define the recommend time step as:

$$T_{\text{ref}} = \frac{1}{5} T_{\text{smallest}} \quad (9)$$

where  $T_{\text{smallest}}$  is the smallest time constant in the network and  $T_{\text{ref}}$  is the recommend time step for the network simulation.

After the analysis of the equivalent circuit model in Fig. 1, we consider the time step selection for each different order network as shown in Fig. 5. From Eq. (8), each time constant that associates with each independent energy storage component (capacitor or inductor) in Fig. 5 can be obtained. From these calculation results, we choose the smallest time constants of each different order network and list them in Table 3. Table 3 also lists the recommend maximum simulation time step for each order according to Eq. (9).

It can be seen from Table 3, if the five-order RC network circuit is adopted, the simulation time step should be set smaller than  $T_{\text{ref}5}$ ; if the four-order network circuit is used, the simulation time step should be limited to the range between  $T_{\text{ref}5}$  and  $T_{\text{ref}4}$ , etc. The maximum simulation time step for this model is  $T_{\text{ref}2}$ . Notice that if a two-order is chosen for simulation, the time step size now is about 0.16s,

Table 3  
The smallest time constant in each order network and the recommend time steps

Different order network	Related components of the smallest time constant	Time constant (s)	Recommend maximum simulation time step (s)
Five-order RC + L	$R_5 - L$	9.8187E–6	$T_{\text{ref}5} = 1.964E-6$
Four-order RC	$(R_5 + R_4) - (C_5 + C_4) - R_3$	0.002596	$T_{\text{ref}4} = 5.192E-4$
Three-order RC	$(R_5 + R_4 + R_3) - (C_5 + C_4 + C_3) - R_2$	0.0688768	$T_{\text{ref}3} = 0.01378$
Two-order RC	$(R_5 + R_4 + R_3 + R_2) - (C_5 + C_4 + C_3 + C_2) - R_1$	0.729579	$T_{\text{ref}2} = 0.145916$

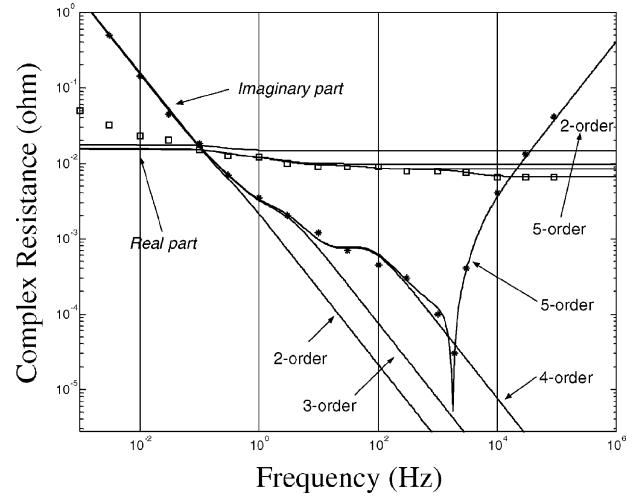


Fig. 6. Comparison of different order model simulation results (—) with measurement ( $\square$  and  $*$ ).

while the original model needs a step size of  $2\mu\text{s}$ . Significant computational time saving is obvious.

#### 2.4. Model order selection

Fig. 6 shows the comparison among different order networks simulation results and the measurements. The five-order fits the whole test frequency spectrum. The imaginary part the complex resistance first decreases as the frequency increases, and then it increases because of the series inductor. The four-, three- and two-order fit the low frequency bands well respectively.

To discuss the merits of the reduced order model, we calculate the complex impedance error between two adjacent orders. As shown in Fig. 6, the error between two consecutive orders increases as the frequency increases. Define this error as:

$$E_{n,(n-1)}(f) = \frac{||Z_{n-1}(f)| - |Z_n(f)||}{|Z_n(f)|} \times 100\% \quad (10)$$

where  $E_{n,(n-1)}(f)$  is the error between order  $n$  and order  $n-1$  at frequency  $f$ ,  $n$  is the order number,  $Z_n$  is the complex impedance and  $f$  is the frequency.

The frequency at which the error exceeds 1% can be calculated according to Eq. (10) and they are listed in Table 4.

Table 5 combines the Tables 3 and 4, which explains the model order selection with maximum 1% truncation error.



Table 4  
Frequency at which error > 1%

Error	1% Error frequency (Hz)
$E_{5-4}$	550
$E_{4-3}$	1.44
$E_{3-2}$	0.0034

Table 5  
Model order selection method

Frequency band of interest (Hz)	Model order	Recommended simulation time step (s)
$f > 550$	6	$T \leq 1.964E-6$
$1.44 < f \leq 550$	4	$1.964E-6 < T \leq 5.192E-4$
$0.0034 < f \leq 1.44$	3	$5.192E-4 < T \leq 0.01378$
$f < 0.0034$	2	$0.01378 < T \leq 0.145916$

For example, if the relevant frequency band of a simulation is wider than 550 Hz, the ultracapacitor model will adopt the five-order RC circuit, and the recommend time step for this simulation is  $T \leq 1.964E-6$  s.

Fig. 7 shows the working frequency band for the different order networks.

2.5. Capacity scaling

Another useful characteristic of this model is capacity scaling. Model default parameter values are based on a Maxwell 100 F ultracapacitor, but the model will automatically calculate new parameters according to users' specified capacitance by using Eq. (11):

$$N = \frac{C_{Total}}{100}, \quad R_{k\_NEW} = \frac{R_k}{N},$$

$$C_{k\_NEW} = C_k \cdot N, \quad L_{NEW} = \frac{L}{N} \tag{11}$$

where  $N$  is the capacity-scaling ratio, and  $R_{k\_NEW}$ ,  $C_{k\_NEW}$  and  $L_{NEW}$  are the new values corresponding to the new

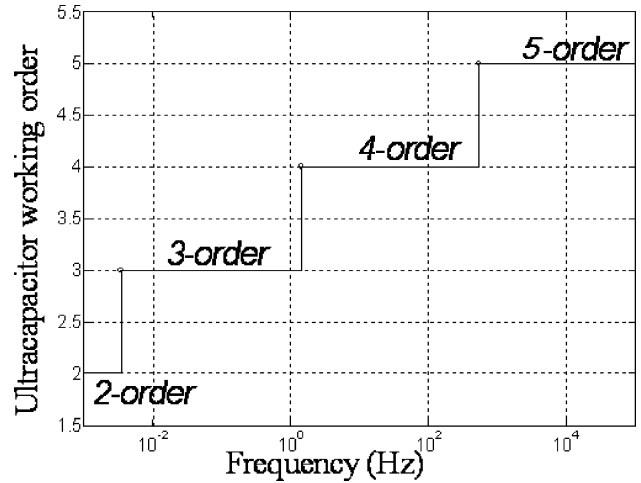


Fig. 7. Working frequency band of different orders.

total capacitance. This scaling is a little risky considering that electrode parameters may change with capacity, but it nonetheless gives a quite good estimate of capacitor performance for system-level studies. Fig. 8 shows the accuracy of scaling the capacity from 100 F (default value) to 10 and 5 F, and comparison with measurements of Maxwell 10 and 5 F capacitors. On the left is the comparison of Maxwell 10 F and on the right is 5 F.

From Fig. 8, we can see that the model with capacity scaling matches well experiments within the same brand product family. Comparison with different brand products may have a larger error.

3. Model used in FCHV simulation

One important application of ultracapacitors is in the fuel cell powered hybrid electric vehicles (FCHVs), in which the ultracapacitor provides peak power during acceleration or serves as the immediate repository for electric energy regenerated during braking. Simulation of a hybrid electric

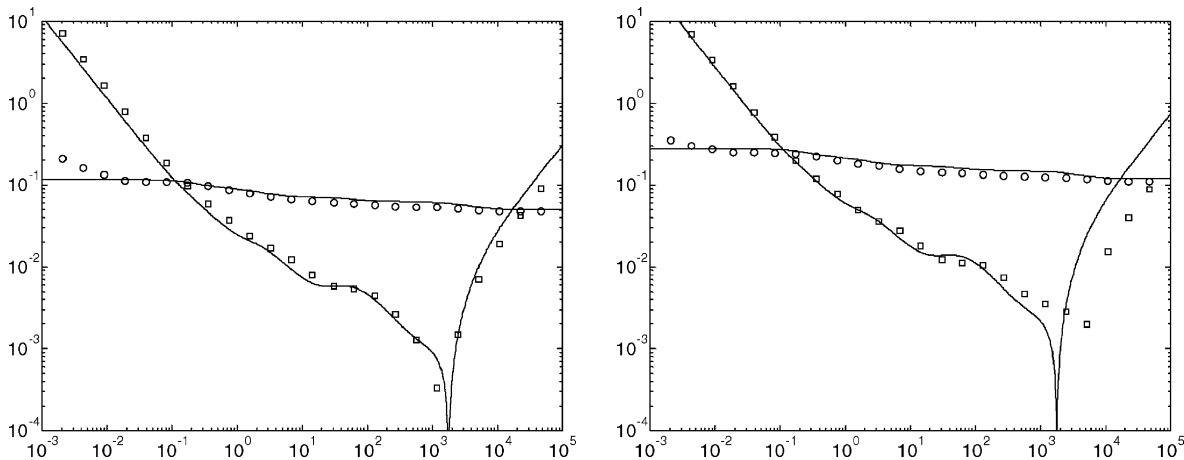


Fig. 8. Comparison between model simulation results (—) and Maxwell ultracapacitor measurements (□ and ○).

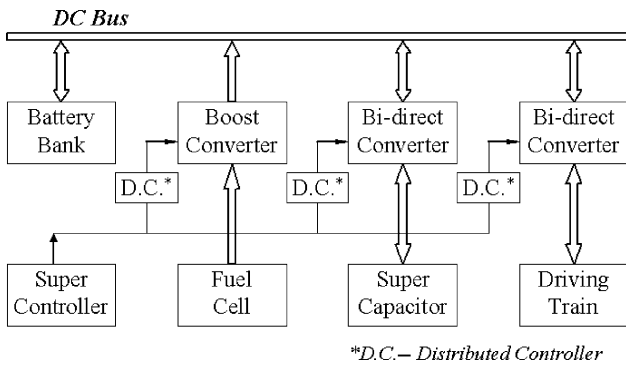


Fig. 9. Block diagram of hybrid electric vehicle.

vehicle is a complex process involving many technical disciplines. The interdisciplinary nature of the problem requires its component models to be accurate, fast and robust.

The FCHV described in this paper is composed of a mechanical train that includes all the mechanical parts of the vehicle, including the motor that converts energy between electrical and mechanical, a fuel cell system as the primary source of power, battery and ultracapacitor stacks to meet high and intense power demands respectively, D.C./D.C. converters to control power flow between the components, and a supervisory controller to control and balance the whole system. Fig. 9 shows the block diagram of the FCHV.

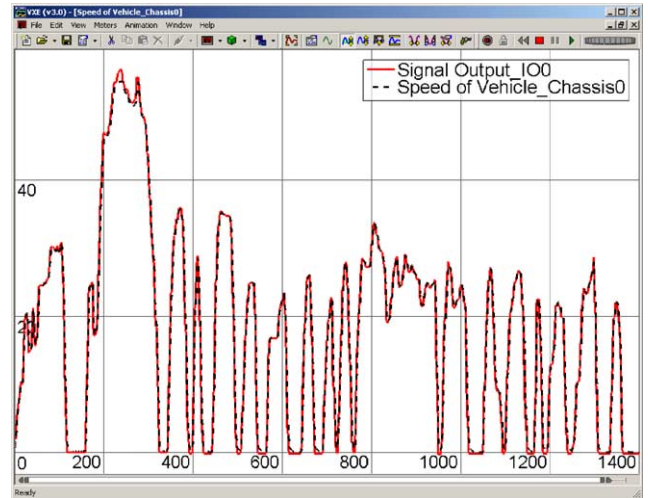


Fig. 11. Speed of vehicle during EPA city driving test.

As shown in Fig. 9, the ultracapacitor bank is connected to the D.C. bus through a bi-directional D.C./D.C. converter, which is controlled by the vehicle supervisory controller. Fig. 10 shows the FCHV system schematic in the VTB environment.

The designed FCHV is tested using the Environmental Protection Agency (EPA) city driving test profile. Some simulation results are shown in Figs. 11 and 12. Fig. 11 shows

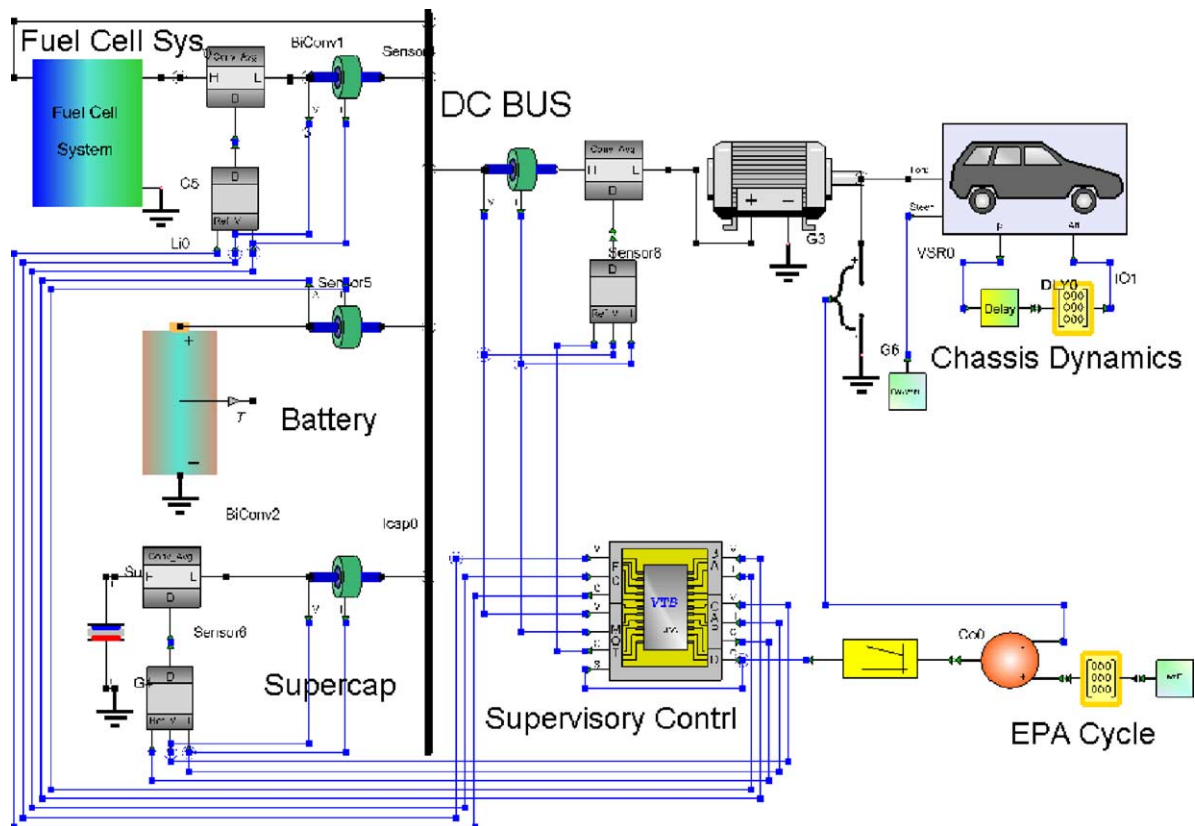


Fig. 10. Schematic of FCHV system in VTB.

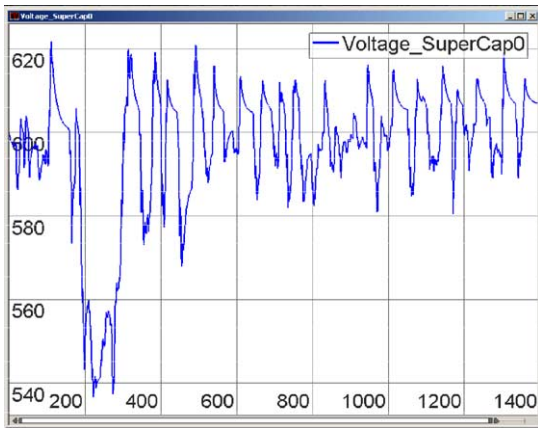


Fig. 12. Terminal voltage of the ultracapacitor bank during EPA city driving test.

the vehicle speed variation during the EPA city driving test with the y-axis as the speed in mil/h and the x-axis as the time in second. It can be seen the vehicle speed (dash curve) follows the commands (solid curve) very well.

Fig. 12 shows the simulation result of the ultracapacitor voltage variation during the EPA city driving test, the y-axis is the voltage in volts and x-axis is the time in seconds. The total capacity of the ultracapacitor model is scaled from 100 to 76 F according to the vehicle energy requirement. The initial value of the ultracapacitor terminal voltage is set as 600 V in order to store more energy and in turn to decrease the usage of ultracapacitors. The ultracapacitor voltage increases to the maximum value about 620 V when the vehicle decelerates, and decreases to about the minimum value about 540 V when the vehicle accelerates.

In this simulation, the simulation time step is set as 0.01 s. According to Table 5, the ultracapacitor works in three-order. The simulation works well without numerical oscillations.

#### 4. Conclusions

A multi-stage resistance/capacitor ladder model has been built with automatic order selection and capacity scaling for ultracapacitor modeling. The feature of the automatic order selection makes the model automatically select the order or number of stages of the ladder network according to the simulation time step to minimize calculation error

and save computational cost. The feature of the capacity scaling makes the model accurately reflect other capacitors with different sizes. A model with automatic order changing up and down while the simulation is running with variable simulation time step, will be explored in future work.

#### Acknowledgements

This work was sponsored by the US Army Communications and Electronics Command under contract NRO-00-C-0134 and by the US Office of Naval Research under contracts N00014-02-1-0623 and N00014-03-1-0434.

#### References

- [1] A. Yoshida, K. Imoto, H. Yodeda, A. Nishino, An electric double-layer capacitor with high capacitance and low resistance, *IEEE Trans. Comp., Hybrid, Manufac. Tech.* 15 (1) (1992) 133–138.
- [2] J. Newman, *Electrochemical Systems*, Prentice-Hall, Englewood Cliffs, NJ, 1991, pp. 454–495.
- [3] V. Srinivasan, C. Lin, J. Ritter, J. Weidner, Mathematical modeling of sol-gel derived carbon xerogels as double layer capacitors, *Electrochem. Soc. Proc.* 25–96 (1996) 153–166.
- [4] C.J. Farahmandi, A Mathematical model of an electrochemical capacitor with porous electrodes, *Electrochem. Soc. Proc.* 25–96 (1996) 167–179.
- [5] J.R. Miller, Battery-capacitor power source for digital communication applications: simulations using advanced electrochemical capacitors, *Electrochem. Soc. Proc.* 29–95 (1995) 246–254.
- [6] A.F. Burke, J.R. Miller, Test procedures for high energy density electrochemical capacitors, *Electrochem. Soc. Proc.* 29–95 (1995) 280–297.
- [7] R.A. Dougal, C.W. Brice, R.O. Pettus, G. Cokkinides, A.P.S. Meliopoulos, virtual prototyping of PCIM systems—the Virtual Test Bed, in: *Proceedings of the PCIM/HFPC 1998 Conference*, Santa Clara, CA, November 1998, pp. 226–234.
- [8] J.R. Miller, Evaluation of capacitors and batteries for pulsed power applications associated with satellite communications. Part 2. capacitor equivalent circuit models and ragon plots, *JME-MRJ2*, JME, October 30, 2000 (private communication).
- [9] F.L. Alvarado, R.H. Lasseter, J.J. Sanchez, Testing of trapezoidal integration with damping for the solution of power transient problems, *IEEE Trans. Power Appar. Syst.* PAS-102 (2) (1983) 3783–3790.
- [10] J.R. Marti, J. Lin, Suppression of numerical oscillations in the EMTP, *IEEE Trans. Power Syst.* 4 (2) (1989) 739–747.
- [11] W. Gao, E. Solodovnik, R. Dougal, G. Cokkinides, A.P.S. Meliopoulos, Elimination of numerical oscillations in power system dynamic simulation, in: *Proceedings of the IEEE Applied Power Electronics Conference*, Miami, USA, 2003.